Relationship among Mechanical Properties Anisotropy, Microstructure and Texture in AA 6111 Alloy Sheets

WANG Xiaofeng[1,2], GUO Mingxing[1*], CAO Lingyong[1], PENG Xiangyang[1], ZHANG Jishan[1], ZHUANG Linzhong[1]

(1. State Key Laboratory for Advanced Metals and Materials, University of Science and Technology Beijing, Beijing 100083, China; 2. Faculty of Mechanical Engineering & Mechanics, Ningbo University, Ningbo 315211, China)

Abstract: We comparatively studied the mechanical properties anisotropy, microstructure and texture of the commercial and the new developed AA6111 alloys through tensile test, optical microscopy, and XRD analysis. The results show that the anisotropy of mechanical properties for the developed AA6111 alloy is lower than that of the commercial alloy. The developed alloy possesses higher r value, lower Δr value and more uniform microstructure, compared with the commercial AA6111 alloy, indicating that the deep drawability of the developed alloy has been improved significantly. The recrystallization textures of the two alloy sheets are also different. The recrystallization texture of the commercial alloy sheet mainly includes Cube and {114}<311> orientations, while the recrystallization texture of developed alloy sheet consists of Cube, Goss and R orientations. The relationships among the deep drawabilities, microstructure and texture were discussed thereafter.

Key words: AA6111 alloy; mechanical properties anisotropy; microstructure; deep drawability; texture

1 Introduction

In recent years, the wide application of Al alloys in automotive body panels, *i e*, 2xxx, 5xxx and 6xxx series Al alloys, has brought a great weight reduction that can reduce fuel consumption and exhaust gas emission. Compared with other Al alloys, such as 2xxx and 5xxx series alloys, 6xxx series alloy sheets stand out by a combination of good formability, good corrosion resistance and satisfactory strengthening potential during paint bake cycles at high temperatures. The potential 6xxx alloys are in use for car body outer panels, including AA6009, AA6010, AA6016, AA6022 and AA6111[1-8]. Among these alloys, European car companies prefer AA6016 alloy as a result of its high formability, while AA6111 alloy possesses higher strength and is interested by US carmakers. The mechanical properties of the typical aluminum alloys used for body panels are summarized in Table 1.

Due to the higher strength of AA6111 alloy, thus, an un-suitable thermomechanical processing results in the bad formability of alloy. It is known that the deep drawability of alloy is greatly influenced by the Lankford value (r value), which is defined as the ratio of the transverse strain to the normal strain[10,11]. It has been experimentally proven that there is a positive correlation between r value and LDR value[12]. Compared with LDR value, r value can be more easily determined only through unidirectional tensile test. Hence, the deep drawability can be characterized by the average r and Δr values which are expressed by:

$$\bar{r} = (r_0 + 2r_{45} + r_{90})/4 \tag{1}$$

$$\Delta r = (r_0 + r_{90} - 2r_{45})/2 \tag{2}$$

where r_0, r_{45}, r_{90} are the values in 0°, 45° and 90° directions with respect to the rolling direction, respectively.

Generally speaking, high average r and low Δr values are beneficial to deep drawing, which mainly depends on crystallographic texture. It is commonly accepted that texture also has some influence on material properties, such as, Young's modulus, strength, ductility, toughness, magnetic permeability, electrical

Table 1 Mechanical properties of automotive aluminum alloys[9]

Alloy	Composition/wt%	Condition	UTS/MPa	YS/MPa	Elongation/%	Average r	Average n
AA6009	0.5Mg-0.8Si	T4	250	130	24	0.64	0.29
AA6016	0.4Mg-1.2Si	T4	210	105	26	0.61	0.3
AA6111	0.7Mg-0.9Si-0.7Cu	T4	290	160	25	0.55	0.28

conductivity and thermal expansion, but here for the Al alloy sheets used in car body panels, the component and intensity of texture normally have a significant effect on the deep drawability of alloy sheets[13]. The mechanical properties contained strengths, ductility and r value of automotive aluminum sheet should be considered. It is very clear that how the texture components affect r value, however, obscure for strength and ductility.

The effect of texture on deep drawability was studied by some researchers[10,12] and it has been repeatedly described that Cube texture and Goss texture possess low average r value and large Δr value respectively which are not beneficial to deep drawability, while γ fibre has large average r and low Δr values, which leads to good deep drawability[14-17]. However, the relationship between the texture and the deep drawability was illustrated not deep, which can be attributed to the fact that r values of some uncommon texture components are still not clear. In order to clarify the effect of texture on the mechanical properties anisotropy especially the deep drawability more deeply, a commercial AA6111 alloy and a new developed AA6111 alloy were studied in this study. The aim of this paper is to compare the differences in mechanical properties anisotropy, microstructure and texture components for these two alloys, and establish the relationship among deep drawability, microstructure and texture.

2 Experimental

The chemical composition of two AA6111 aluminum alloys is given in Table 2. The 1 mm thickness commercial and our developed AA6111 sheets which are denoted A, B respectively have been solution treated at 555 ℃ for 2 min in salt bath furnace, and then pre-aged at 80 ℃ for 12 hours plus naturally aged for 14 days (T4P state).

The mechanical properties of the alloy sheets

Table 2 Chemical composition of the two AA6111 Al alloys/wt%

Alloy	Mg	Si	Cu	Mn	Fe	Al
A	0.6	0.8	0.65	0.2	0.25	balance
B	0.8	0.9	0.5	0.1	0.2	balance

at T4P state, including yield strength (YS), ultimate tensile strength (UTS), elongation, n and r values, were measured at room temperature in three directions, as shown in Fig.1. Among the above parameters, r value was determined by a tensile strain of 15%.
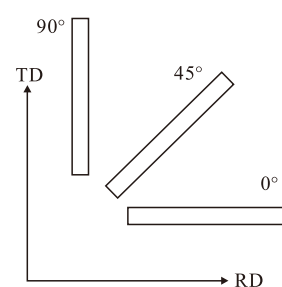
Fig.1 Diagram of cutting way for the tensile test samples

Optical microscope was used to observe the microstructure. The standard metallographic techniques and Keller's reagent were used for the optical microscopical observation.

To analyze the recrystallization texture of the sheets, {111},{200},{220} and {311} incomplete pole figures were measured by D5000 X-ray gonimeter using Cu_Kα radiation. Orientation distribution functions (ODFs) were calculated from four incomplete pole figures by the series expansion method with l_{max}=22. The dimension of specimen was 24 mm(rolling direction)×14 mm(transverse direction).

3 Results and discussion

3.1 Mechanical properties

The mechanical properties of the two alloys in the different directions are presented in Fig.2. It can be easily seen that their mechanical properties are different in the three directions, indicating that they are both anisotropic. However, alloy B has lower mechanical properties anisotropy as a result of the slighter differences of mechanical properties in the three directions. According to the detailed mechanical properties of alloy sheets A and B shown in Table 3, it can be clearly seen that the strengths of alloy A in the three directions are all higher than those of alloy B in the corresponding directions, but the elongation of alloy A in the rolling direction is the lowest. In

addition, alloy B possesses the higher r value and lower Δr value compared with alloy A, indicating that the anisotropy of alloy B has been controlled better thus it may have better deep drawability.
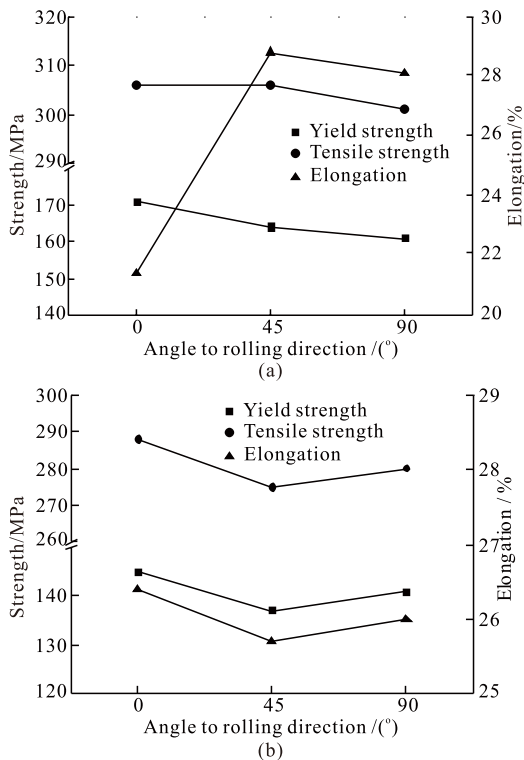
Fig.2 Strength and elongation of AA 6111 sheets at T4P state in the 0°, 45°, 90° directions: (a) sheet A; (b) sheet B

According to the results, it can be seen that the chemical composition may have a strong influence on the mechanical properties anisotropy. The new developed alloy B possesses very high r value and elongation similar to those of AA6016 and low strength similar to that of AA6009. It can be concluded that alloy B almost has the same deep drawability as AA6016.

As mentioned above, LDR is a specific parameter to evaluate deep drawability. Leu[18] pointed out that LDR depends on both r value and n value. Sidor[12] pointed out that LDR value mainly depends on the r value to a large extent but the effect of n value is less. The LDR usually can be expressed as follows:

$$LDR = \sqrt{\exp\left[\left(2f\exp\left(-n\right)\right)\sqrt{\frac{1+\bar{r}}{2}}\right] + \exp\left[2n\sqrt{\frac{1+\bar{r}}{2}}\right]} - 1$$

$$(3)$$

where f is the factor of drawing efficiency, and when f equals 0.9, the calculated results should be much more accurate. Thus, the *LDR* values of the alloys A and B can be calculated according to the average r and n values. The *LDR* values are 1.99 and 2.01 respectively.
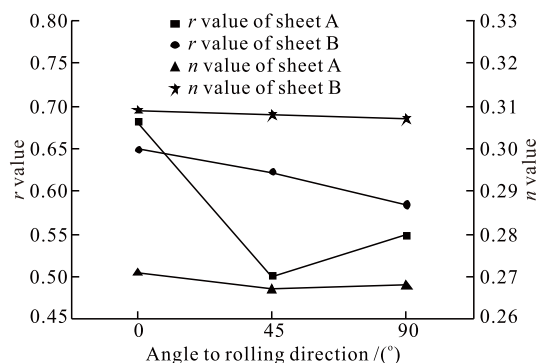
Fig.3 Planar anisotropy of n and r values of sheets A and B in the 0°, 45°, 90° directions

The anisotropies observed from the two alloy sheets are presented in Fig.3. The difference of r values between alloys A and B should result from the different recrystallization textures. Therefore, the following part will give a detailed discussion on the microstructure and texture.

3.2 Microstructure

It is known that the mechanical property anisotropy is also related to the microstructure. In order to deeply understand the differences in the mechanical properties of alloys A and B, it is necessary to analyze their microstructures. The microstructure of alloy A is shown in Fig.4. It can be seen that there are lots of slightly elongated recrystallization grains in the alloy and the average size of the grains is about 22 μm. The grains are somewhat longer along the longitude than the transverse direction. This probably is one of the reasons why the alloy has significant mechanical

Table 3 Mechanical properties anisotropy of the two sheets at T4P state

AA 6111	Direction/(°)	YS/MPa	UTS/MPa	Elongation/%	n	Average n	r	Average r	Δr
A	0	171	306	21.4	0.271		0.681		
	45	164	306	28.8	0.267	0.268	0.501	0.558	0.114
	90	161	301	28.1	0.268		0.549		
B	0	145	288	26.4	0.309		0.649		
	45	137	275	25.7	0.308	0.308	0.623	0.62	−0.006 5
	90	141	280	26	0.307		0.584		

Journal of Wuhan University of Technology-Mater. Sci. Ed. www.jwutms.net June 2016

651

properties anisotropy. In addition, the microstructures of the surface layer and center parts are different, which can be clearly seen in Figs.4(a) and (c). It should result from the different deformation and recrystallization behaviors. As is shown in Figs.4(b) and (d), some fine particles can also be observed in the recrystallization grains. According to the recrystallization grain growth theory in Ref.[19], the particles distributing in the alloy matrix can have a significant effect on the deformation and recrystallization behaviors and texture evolution of the alloys during the deformation and heat treatment. Therefore, the observed particles should also affect the texture evolution.
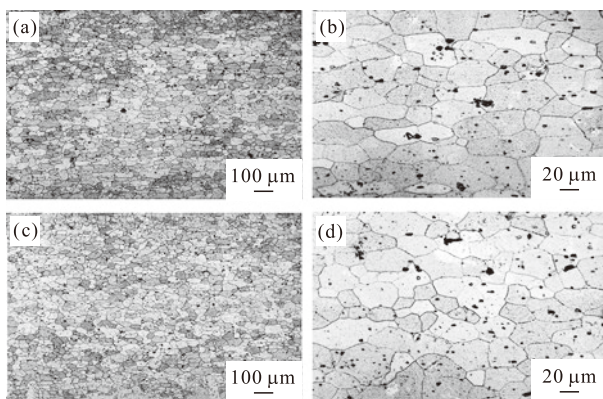
Fig. 4 Recrystallization microstructure of alloy A: (a) longitudinal section; (b) surface layer in longitudinal section; (c) transverse section; (d) surface layer in transverse section
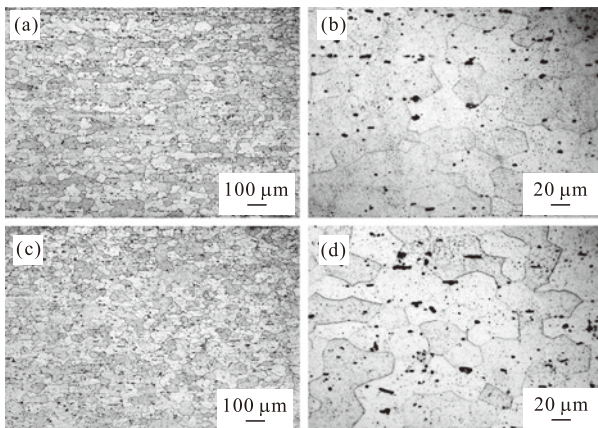
Fig.5 Recrystallization microstructure of alloy B: (a) longitudinal section; (b) surface layer in longitudinal section; (c) transverse section; (d)surface layer in transverse section

The microstructure of alloy B is shown in Fig.5. The microstructure of alloy B is similar to that of alloy A. However, compared with alloy A, alloy B is composed of a more uniform through-thickness microstructure and the grains aspect ratio of the longitudinal grains is smaller that can reduce mechanical properties anisotropy. In addition, the

average grain size with a value of 35 μm for alloy B is larger, and this can also result in a lower strength except the chemical composition.

3.3 Recrystallization texture

The recrystallization texture of the two alloy sheets is shown in Fig.6. The recrystallization texture of the alloy A mainly includes Cube {001}<100> and {114}<311> orientations with the intensities of 7.7 and 5.4 respectively. In alloy B, the recrystallization texture components change slightly, mainly including Cube, Goss {110}<001> and R {124}<211> orientations with the intensities of 10.9, 2.9 and 3.2, respectively.
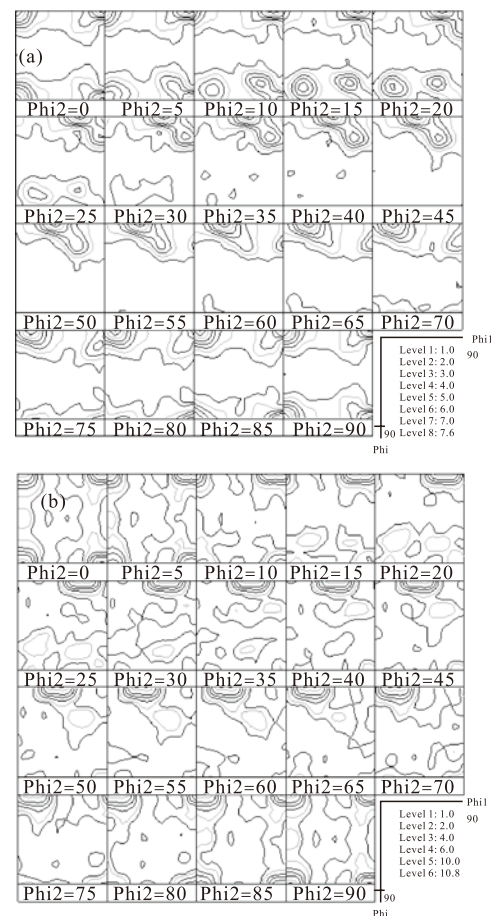
Fig.6 ODFs of the two alloy sheets after pre-aging treatment (a) alloy A; (b) alloy B

Obviously, there are some differences in texture components between two alloy sheets, which will result in the different mechanical properties anisotropy.

It is well known that the recrystallization behaviour of particle containing Al alloys depends on the precipitation state: large (>1 μm) particles will act as sites to promote recrystallization and tend to form random texture, whereas small (<1 μm) particles will pin on the boundaries and retard their movements and Cube bands will act as site to form Cube orientation[19]. Based on the above recrystallization texture results,

it can be concluded that massive small particles precipitated during the thermomechanical processing, thus the PSN effect was strongly suppressed during the recrystallization.

In addition, a metastable {114}<311> orientation in sheet A is attributed to the {114}<311> nuclei which have not been completely consumed by another preferred nuclei such as Cube, Goss and *R* during recrystallization growth stage. Hence, it can be inferred that sheet A was at continuous growth stage, while sheet B had a complete recrystallization.

According to the results mentioned above, it can be seen that the mechanical properties anisotropy especially deep drawability is not only related to the microstructure, but also related to the texture. The *r* and Δ*r* values can be improved by optimizing the texture. It has been also reported that even only one single texture component contained in an alloy, the *r* values in different directions are also different. If one alloy contains several different texture components, its *r* value normally can be calculated by the following Eq.[20]:

$$r = \sum V_j r_j \qquad (4)$$

where r_j is the *r* value of single crystal in the *j*-th orientation, V_j is the volume fraction of the *j*-th orientation. In addition, it has been reported that the relationship between intensity and volume fraction of texture can be expressed as follows[21]:

$$V_j = \frac{1}{2\sqrt{\pi}} Z_j S_0^j \psi_j \left[1 - \exp\left(-\frac{\psi_j^2}{4} \right) \right] \qquad (5)$$

where *Z* is the repeat times of a certain orientation, S_0^j is the central intensity of the *j* texture component of Gaussian distribution, ψ_j is the angle that deviates from the center when the intensity decreases from S_0^j to S_0^j/e.

Table 4 Volume fractions of the recrystallization texture components in the two sheets

AA 6111	Texture component	Intensity	Volume fraction/%
A	Cube{100}<001>	7.7	63
	{114}<311>	5.4	37
B	Cube{100}<001>	10.9	64.1
	Goss{110}<001>	2.9	16.8
	R{124}<211>	3.2	19.1

According to Eq.(5), it could be found that the volume fraction is strongly influenced by the intensity and deviation angle of texture component. Random and other low intensity components have been ignored, thus

the calculated results listed in Table 4 are approximate results. The calculated results reveal that the volume fraction is proportional to the texture intensity.

Table 5 Simulated average *r* and Δ*r* values for some texture components

Texture component	Average *r*	Δ*r*
Cube{100}<001>	0.5	1
Goss{110}<001>	15	30
R{124}<211>	1.9	−1.2
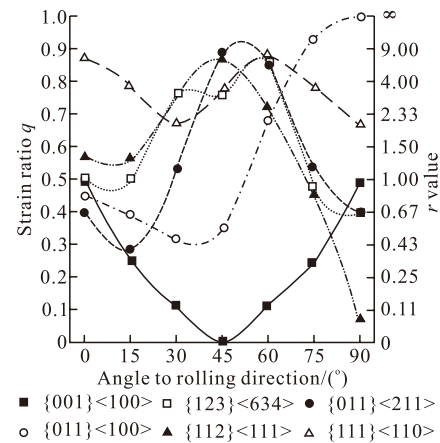
Fig.7 Strain ratio *q* and *r* value calculated by Tailor model[9]

Sidor[22] once calculated the average r and Δ*r* values for some texture components using Taylor model, with the results shown in Table 5. According to his results, both the average r and Δ*r* values for Goss orientation are the highest, but the average *r* and Δ*r* values for the Cube orientation are the lowest. Accordingly, we can see that one single Cube orientation or Goss orientation is not beneficial to improve the deep drawability of alloy. Actually, the *r* values of one single texture component are quite different in different directions, Cube orientation and Goss orientation normally can produce a V-shaped profile (as shown in Fig.7), while R, Copper, S and B orientations can produce inverse V-shaped profile. If the alloy includes several texture components, its average *r* and Δ*r* values can be calculated through Eq. (1), Eq.(2), Eq.(4) and Eq.(5). However, it is also difficult to obtain the accurate result by the theoretical calculation alone. Thus, the larger average *r* value of alloy B (as shown in Table 3) should be attributed to the Goss orientation, and the combination of Goss and other texture components finally results in the lower Δ*r* value. In addition, although the formation of {114}<311> orientation appeared in alloy A is still unknown in this work, according to the average *r* and Δ*r* values (as shown in Table 3), the {114}<311> orientations should be not beneficial to the improvement of deep drawability.

Based on the above analysis, it can be concluded that even Cube and Goss orientations are detrimental to the improvement of deep drawability, but the final deep drawability is not bad because the deep drawability mainly depends on the combination of all the texture components and their corresponding volume fractions. Therefore, it is important to balance the texture components and volume fractions of them.

4 Conclusions

In order to establish the relationship among mechanical properties anisotropy, microstructure and texture for the AA6111 alloy sheets, the differences in the mechanical properties, microstructure and texture for the commercial and new developed AA6111 alloys were discussed in details. The results are summarized as follows:

a) The mechanical properties anisotropy of the developed AA6111 alloy is lower than that of the commercial alloy. The developed alloy possesses higher r value, lower Δr value and more uniform microstructure compared with commercial AA6111 alloy, which indicates that the deep drawability of the developed alloy has been improved significantly.

b) The recrystallization microstructures of the two alloy sheets are composed of slightly elongated grains. The different aspect ratios of the grains in the two alloy sheets help to explain the mechanical properties anisotropy. The average grain size of the commercial alloy is smaller than that of the developed alloy.

c) The recrystallization texture of the commercial alloy sheet mainly includes Cube and {114}<311> orientations, while the recrystallization texture of the developed alloy sheet consists of Cube, Goss and R orientations. It is found that the deep drawability of alloy mainly depends on the combination of all texture components.

References

[1] Burger G B, Gupta A K, Jeffrey P W, *et al*. Microstructural Control of Aluminum Sheet Used in Automotive Applications [J]. *Mater. Charact*., 1995, 35(1): 23-39

[2] Hirsch J, Al-Samman T. Superior Light Metals by Texture Engineering: Optimized Aluminum and Magnesium Alloys for Automotive Applications [J]. *Acta Mater*., 2013, 61(3): 818-843

[3] Sidor J J, Petrov R H, Kestens L A I. Modeling the Crystallographic Texture Changes in Aluminum Alloys during Recrystallization [J]. *Acta Mater*., 2011, 59(14): 5 735-5 748

[4] Engler O, Hirsch J. Texture Control by Thermomechanical Processing of AA6xxx Al-Mg-Si Sheet Alloys for Automotive Applications-a Review [J]. *Mater. Sci. Eng*., 2002, A336: 249-262

[5] Sidor J, Miroux A, Petrov R, *et al*. Controlling the Plastic Anisotropy in Asymmetrically Rolled Aluminium Sheets [J]. *Philos. Mag*., 2008, 88(30-32): 3 779-3 792

[6] Liu H, Song W J, Zhao G, *et al*. Effect of Mg on Microstructures and Properties of Al-Mg-Si-Cu Aluminium Alloys for Automotive Body Sheets [J]. *Trans. Nonferrous Met. Soc. China*, 2005, 15(1): 30-34

[7] Ghosh M, Miroux A, Werkhoven R J, *et al*. Warm Deep-drawing and Post Drawing Analysis of Two Al-Mg-Si Alloys [J]. *J. Mater. Process. Technol*., 2014, 214(4): 756-766

[8] Hu Z Q, Wan L, Wu S S, *et al*. Microstructure and Mechanical Properties of High Strength Die-casting Al-Mg-Si-Mn Alloy [J]. *Mater. Des*., 2013, 46: 451-456

[9] Inoue H, Takasugi T. Texture Control for Improving Deep Drawability in Rolled and Annealed Aluminum Alloy Sheets [J]. *Mater. Trans*., 2007, 48(8): 2 014-2 022

[10] Davies G. *Materials for Automobile Bodies* [M]. Pergamon: Oxford, 2004

[11] Inoue H, Yamasaki T, Gottstein G, *et al*. Recrystallization Texture and *r*-value of Rolled and T4-treated Al-Mg-Si Alloy Sheets [J]. *Mat. Sci. Forum*, 2005, 495-497: 573-578

[12] Sidor J, Petrov R, Kestens L. Deformation, Recrystallization and Plastic Anisotropy of Asymmetrically Rolled Aluminum Sheets [J]. *Mat. Sci. Eng*., 2010, A528: 413-424

[13] Engler O, Randle V. *Introduction to Texture Analysis, 2nd ed*. [M]. London: CRC Press, 2009

[14] Wu P D, Macewen S R, Lloyd D J, *et al*. Effect of Cube Texture on Sheet Metal Formability [J]. *Mat. Sci. Eng*., 2004, A364: 182-187

[15] Jin H, Lloyd D J. Evolution of Texture in AA6111 Aluminum Alloy after Asymmetric Rolling with Various Velocity Ratios between Top and Bottom Rolls [J]. *Mat. Sci. Eng*., A465: 267-273

[16] Engler O, Kim H C, Huh M Y. Formation of {111}Fibre Texture in Recrystallised Aluminium Sheet [J]. *Mat. Sci.Technol*., 2001, 17(1): 75-86

[17] Singh R K, Singh A K, Prasad N E. Texture and Mechanical Property Anisotropy in an Al-Mg-Si-Cu Alloy [J]. *Mat. Sci. Eng*., 2000, A277: 114-122

[18] Leu D. Prediction of the Limiting Drawing Ratio and the Maximum Drawing Load in Cup-drawing [J]. *Int. J. Mach. Tool. Manu*., 1997, 37(2): 201-213

[19] Engler O, Vatne H E, Nes E. The Roles of Oriented Nucleation and Oriented Growth on Recrystallization Texture in Commercial Purity Aluminium [J]. *Mat. Sci. Eng*., 1996, A205: 187-198

[20] Liu Y S, Kang S B, Ko H S. Texture and Plastic Anisotropy of Al-Mg-0.3Cu-1.0Zn Alloys [J]. *Scripta Mater*., 1997, 37(4): 411-417

[21] Bung H J. *Texture Analysis in Material Science* [M]. London: Butterworths Press, 1982

[22] Sidor J, Miroux A, Petrov R, *et al*. Microstructural and Crystallographic Aspects of Conventional and Asymmetric Rolling Processes [J]. *Acta Mater*., 2008, 56(11): 2 495-2 507